Published in final edited form as:
Org Lett. 2005 November 10; 7(23): 5261–5264. doi:10.1021/ol052121f.

Antineoplastic Diterpene–Benzoate Macrolides from the Fijian Red Alga *Callophycus serratus*

Julia Kubanek[*,†,‡], **Anne C. Prusak**[†], **Terry W. Snell**[†], **Rachel A. Giese**[‡], **Kenneth I. Hardcastle**[§], **Craig R. Fairchild**[‖], **William Aalbersberg**[⊥], **Carmen Raventos-Suarez**[‖], and **Mark E. Hay**[†]

School of Biology and School of Chemistry and Biochemistry, Georgia Institute of Technology, Atlanta, Georgia 30332, Department of Chemistry, Emory University, Atlanta, Georgia 30322, Bristol-Myers Squibb Pharmaceutical Research Institute, Princeton, New Jersey 08543, and Institute of Applied Sciences, University of the South Pacific, Suva, Fiji

Abstract

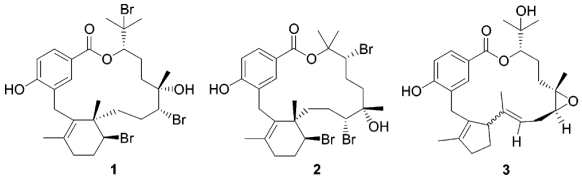

Three diterpene–benzoate natural products, with novel carbon skeletons and an unusual proposed biosynthesis, were isolated from extracts of the Fijian red alga *Callophycus serratus* and identified by a combination of X-ray crystallographic, NMR, and mass spectral analyses. Bromophycolide A (1) displayed cytotoxicity against several human tumor cell lines via specific apoptotic cell death. This represents the first discovery of natural products incorporating a diterpene and benzoate skeleton into a macrolide system.

The discovery of novel carbon skeletons in natural products research is uncommon, providing new targets for synthetic chemists and pharmacologists, and leading to testable hypotheses regarding biosynthetic mechanisms and ecological function. Red macroalgae are well-known for the production of brominated metabolites, including terpenoids and phenols, yet some taxa within the Rhodophyta remain relatively unstudied. Only six secondary metabolites, one oxylipin and five bromophenols, have been previously characterized from the red algal family Solieriaceae.[1,2] Herein, we report the discovery of a unique structural class of macrolides from *Callophycus serratus*, an understudied member of the Solieriaceae. We used bioassay-guided fractionation followed by spectroscopic and X-ray crystallographic analyses to identify three novel natural products (**1**–**3**) of unusual biosynthetic origin and possessing promising antineoplastic and antimicrobial activities.

[*]julia.kubanek@biology.gatech.edu.
[†]School of Biology, Georgia Institute of Technology.
[‡]School of Chemistry and Biochemistry, Georgia Institute of Technology.
[§]Emory University.
[‖]Bristol-Myers Squibb Pharmaceutical Research Institute.
[⊥]University of the South Pacific.

Supporting Information Available: Additional acknowledgments, experimental details, 2D NMR data (COSY, HSQC, HMBC, NOESY, ROESY), ^{1}H NMR spectra for **1**–**3**, and X-ray crystallographic data (tables and CIF files) for **1** and **2**. This material is available free of charge via the Internet at http://pubs.acs.org.

Extracts from *C. serratus* collected at several sites in Fiji were separated by liquid–liquid partitioning and chromatography, guided by a cytotoxicity assay using ingestion rates of the invertebrate *Brachionus calyciflorus* (Rotifera).[3] Following reversed- and normal-phase HPLC, bromophycolides A–B (**1**–**2**) and debromophycolide A (**3**) were isolated (see the Supporting Information for experimental details).[4]

The most abundant natural product from *C. serratus*, bromophycolide A (**1**), displayed an $[M - H]^-$ molecular ion with *m*/*z* 661.0194 and characteristic tribrominated isotopic pattern, suitable for a molecular formula of $C_{27}H_{37}O_4Br_3$. X-ray diffraction analysis of **1** revealed a 15-membered macrolide within a diterpene–benzoate framework (Figures 1 and 2). The bromine atom within the isopropyl appendage was disordered with respect to the isopropyl methyls over two primary positions, with 70% and 30% occupancies. The Flack parameter was refined to be −0.002(16), indicating that the geometry shown is the absolute configuration.

The NMR spectral data of **1** supported the structure derived from X-ray diffraction analysis (Table 1; Supporting Information). HMBC correlations from the methyl groups anchored the carbon skeleton, enabling assignments of all quaternary carbons. COSY and additional HMBC correlations provided the connectivity within spin systems (Supporting Information).

From high-resolution mass spectral data, bromophycolide B (**2**) appeared to be an isomer of **1**, with a parent ion with *m*/*z* 661.0191. X-ray diffraction analysis of **2** indicated a 16-membered macrolide with absolute stereochemistry predicted as in Figures 1 and 2. Chemical shift and 2D NMR correlation data were very similar for most of **1** and **2** (Table 1; Supporting Information), except near the link between benzoate and the diterpene head. In **2**, a downfield-resonating quaternary carbon (C-15; δ 83.4) appeared to be the site of benzoate attachment.

With an $[M - H]^-$ parent ion at *m*/*z* 439.2490 and no characteristic bromine isotope splitting, debromophycolide A (**3**) possessed the molecular formula $C_{27}H_{36}O_5$. Examination of chemical shifts, scalar couplings, and 2D NMR spectral data indicated that the *p*-hydroxybenzoate group was intact (Table 1; Supporting Information). The ester group appeared to be attached to the diterpene skeleton with the same connectivity and stereochemistry as **1**, due to the presence of a downfield methine signal assigned to position 15 of **3** (^{1}H δ 4.96 doublet of doublets; ^{13}C δ 81.7). Two methyl singlets (Me-26: δ 1.23; Me-27: δ 1.24) showed HMBC correlations to C-15, to C-25, and to each other (δ 25.2, 26.4). The downfield resonance for the fully substituted C-25 (δ 72.6) indicated the attachment of OH at that position, leaving one oxygen atom from the molecular formula to be assigned. Chemical shifts for positions 11 (^{1}H δ 2.91; ^{13}C δ 59.8) and 12 (^{13}C δ 59.0) supported the existence of an epoxide group in **3**. NOEs observed between H-10b (δ 2.12) and H-11, between H-10a (δ 1.72) and Me-24 (δ 1.17), but not between H-11 and Me-24 established a *trans* (11*S*,12*S*) configuration at the epoxide within **3** (Supporting Information).

The molecular formula of **3** indicated 10 sites of unsaturation, of which 6 were accounted for by the *p*-hydroxybenzoate and the epoxide. In addition to the aryl group, there were four olefinic carbon resonances accounting for two of these sites, leaving two additional rings, as expected for bromophycolide-type molecules. Working from the epoxide of **3**, H-11 showed COSY correlations with the two methylene H-10 (δ 1.72, 2.12), which in turn both correlated with an olefinic proton H-9 (δ 5.28). The singlet Me-23 (δ 0.93) showed HMBC correlations to C-7 (δ 59.8), C-8 (δ 138.2), and C-9 (δ 122.8), establishing an olefin at positions 8 and 9. From NOEs observed between H-7 (δ 3.31) and H-9, and between H-10b and Me-23, this olefin possessed an *E* configuration. Continuing with the connectivity

analysis, H-7 showed COSY correlations with both methylene H-21 (δ 1.59, 1.91), which in turn showed COSY correlations with both methylene H-20 (δ 2.33, 2.39), to connect C-7 to C-21 and C-21 to C-20. This ended another spin system, but HMBC correlations from Me-22 (δ 1.92) to C-20 (δ 37.5), to C-6 (δ 133.0) and to C-19 (δ 138.0), revealed the position of the last olefin at C-6-C-19. Finally, HMBC correlations from methylene H-5b (δ 3.58) to C-4 (δ 124.3) of the aryl system, and from H-5b to C-7, confirmed the cyclopentenyl group within the larger macrolide framework of **3**. Additionally, weak COSY correlations between H-5a (δ 3.24) and H-20a, and between H-5a and Me-22 provided additional evidence for this connectivity.

Determination of stereochemistry at C-7 of **3** was not straightforward. One would expect an NOE to be observed between H-7 and the *pro-R* H-5 (the one pointing up in Figure 1) if the configuration was 7*S*; such an NOE was not observed. NOEs observed between H-7 and both H-20 could be explained by either configuration at C-7. The broad multiplet resonance of H-7, suggesting small scalar couplings or the lack of a defined conformation for the cyclopentenyl system, offered no additional insights. At this time, the stereochemistry at position 7 remains undetermined.

The three novel macrolides characterized in this study represent two new carbon skeletons, each possessing a hybrid diterpene–benzoate structure. Although diterpene–benzoates have been previously described, for example, tolypodiol from cyanobacteria,[5] to our knowledge, the current study is the first account of such natural products displaying a macrocyclic system.

In the biosynthesis of bromophycolides, carbon–carbon bond formation between benzoate and geranylgeranyl diphosphate (GPP) would be expected to occur by electrophilic aromatic substitution. Esterification could occur either by nucleophilic attack of the benzoyl carboxylate on a bromonium ion-type intermediate of GPP or by transesterification of *p*-hydroxybenzoyl CoA with a bromohydrin intermediate of GPP acting as nucleophile, leading to both 15-membered and 16-membered macrolide products. Bromine atoms were extensively observed within the diterpene fragments of **1**–**2**, positioned at sites that would have been unsaturated within the diterpene precursor, suggesting that halogenation occurred using an electrophilic source of bromine, consistent with previously proposed mechanisms.[6,7] Nucleophilic displacement of Br by OH would lead to the *trans* epoxide evident in **3**. However, in previously identified brominated natural products, regioselectivity and stereoselectivity of biological bromohydrin formation appears to more typically led to *anti* relationships between halogens and OH (although *syn*-substituted bromo- and chlorohydrins are known).[6–8] Cyclization within the diterpene fragment leading to **1**–**3** could have occurred either before or after electrophilic aromatic substitution, according to the mechanism proposed in Scheme 1, consistent with previously proposed mechanisms.[7] The structural similarity of **3** to the bromophycolides suggests that **3** may have been formed as a rearrangement product of a metabolite related to **1** (Scheme 1) or from a common biosynthetic precursor.

Bromophycolide A (**1**) demonstrated moderate in vitro cytotoxic potency (mean panel IC_{50} value: 6.7 uM) and broad activity against a range of tumor types, whereas **2**–**3** demonstrated less potent cytotoxicity values (Table 2). When A2780 human ovarian cells were treated for 24 h with **1**, arrest in the G1 phase of the cell cycle was observed, consistent with loss of cells from the S and G2/M phase (Table 3). In addition, a 10-fold induction of apoptosis occurred as a result of treatment with **1**, with data indicating that apoptosis stemmed from cells arrested in G1.

Bromophycolides A (**1**) and B (**2**) also exhibited moderate antibacterial activity, against methicillin-resistant *Staphylococcus aureus* (MRSA) and vancomycin-resistant *Enterococcus faecium* (VREF), and antifungal activity against amphotericin B-resistant *Candida albicans* (Table 2). Only **1** was isolated in sufficient yield for testing against HIV, revealing anti-HIV IC_{50}s of 9.1 and 9.8 μM for two HIV strains (Table 2).

The current study reports a class of natural products, involving mixed biosynthesis, that is unexpected for red macroalgae. Red algae are widely known as sources of isoprenoid natural products, including halogenated monoterpenes, sesquiterpenes, and diterpenes, as well as being prolific sources of halogenated phenols.[9] Macrocyclic lac-tones derived from isoprenoid biosynthetic precursors are less common, whether from red algae or other natural sources. Our discovery of natural products **1**–**3** representing two new carbon skeletons suggests that members of the red algal family Solieriaceae may possess more active secondary metabolic pathways than previously thought, directing common terpene biosynthetic precursors into unusual macrocyclic natural products.

Supplementary Material

Refer to Web version on PubMed Central for supplementary material.

Acknowledgments

This research was supported by an ICBG grant from Fogarty International Center at the NIH, with supplemental funding from the Teasley Endowment to Georgia Tech. We thank the Government of Fiji for permission to perform research in their territorial waters, and the people of Kadavu, Nadroga, and Rewa provinces for facilitating this work.

References

(1). Graber MA, Gerwick WH, Cheney DP. Tetrahedron Lett. 1996; 37:4635–4638.

(2). Whitfield FB, Helidoniotis F, Shaw KJ, Svoronos D. J. Agric. Food Chem. 1999; 47:2367–2373. [PubMed: 10794638]

(3). Snell, TW. Small-Scale Freshwater Environment Toxicity Test Methods. Blaise, C.; Ferard, JF., editors. Dordrecht; Kluwer: 2005.

(4). Bromophycolide A (**1**): white crystals recrystallized from methanol (39.7 mg; 0.80% plant dry mass); $[\alpha]^{23}_{D}$ −35 (*c* 0.21 g/100 mL, $CHCl_3$); UV (MeOH) λ_{max} 229 nm (log ϵ = 3.73), 265 nm (log ϵ = 4.27); IR (thin film) ν_{max} 3350 (br), 2970, 2930, 1683-1721, 1608, 1455, 1372, 1338, 1265, 1246, 1108, 769, 738 cm^{-1}; ^1H NMR ($CDCl_3$, 500 MHz) and ^{13}C/DEPT NMR ($CDCl_3$, 125 MHz) data, Table 1; NOE, COSY, HMBC NMR data, Supporting Information; HRESIMS $[M - H]^-$ *m*/*z* 661.0194 (calcd for $C_{27}H_{36}O_4Br_3$, 661.0169). Bromophycolide B (**2**): white crystals recrystallized from aqueous methanol (6.1 mg; 0.11% plant dry mass); $[\alpha]^{23}_{D}$ −1 (*c* 0.044 g/100 mL, $CHCl_3$); UV (MeOH) λ_{max} 224 nm (log ϵ = 3.63), 265 (log ϵ = 3.68); ^1H NMR ($CDCl_3$, 500 MHz) and ^{13}C/DEPT NMR ($CDCl_3$, 125 MHz) data, Table 1; NOE, COSY, HMBC NMR data, Supporting Information; HRESIMS $[M - H]^-$ *m*/*z* 661.0191 (calcd for $C_{27}H_{36}O_4Br_3$, 661.0169). Debromophycolide A (**3**): white amorphous solid (1.6 mg; 0.043% plant dry mass); $[\alpha]^{23}_{D}$ −7 (*c* 0.012 g/100 mL, $CHCl_3$); UV (MeOH) λ_{max} 265 nm (log ϵ = 3.46); ^1H NMR ($CDCl_3$, 500 MHz) and ^{13}C/DEPT NMR ($CDCl_3$, 125 MHz) data, Table 1; NOE, COSY, HMBC NMR data, Supporting Information; HRESIMS $[M - H]^-$ *m*/*z* 439.2490 (calcd for $C_{27}H_{35}O_5$, 439.2490).

(5). Prinsep MR, Thomson RA, West ML, Wylie BL. J. Nat. Prod. 1996; 59:786–788. [PubMed: 8792625]

(6). Murphy CD. J. Appl. Microbiol. 2003; 94:539–548. [PubMed: 12631188]

(7). Butler A, Carter-Franklin JN. Nat. Prod. Rep. 2004; 21:180–188. [PubMed: 15039842]

(8). Gribble GW. Chem. Soc. Rev. 1999; 28:335–346.

(9). Blunt JW, Copp BR, Munro MH, Northcote PT, Prinsep MR. Nat. Prod. Rep. 2005; 22:15–61. [PubMed: 15692616]

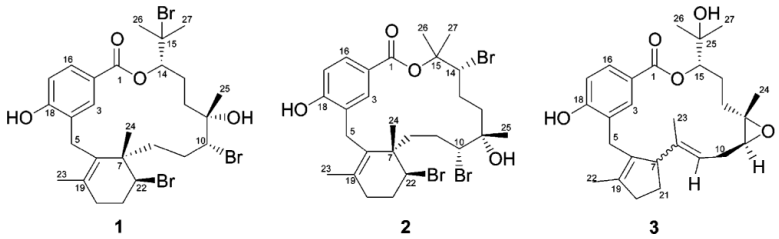

Figure 1.
Novel natural products of *Callophycus serratus.*

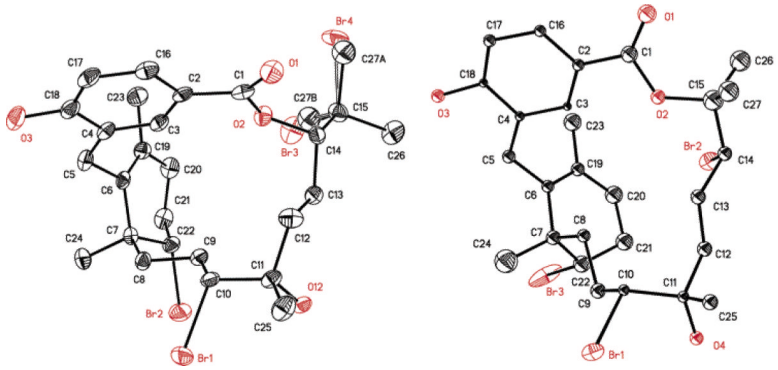

Figure 2.
Perspective drawings of **1** (left) and **2** (right) from X-ray crystallographic data.

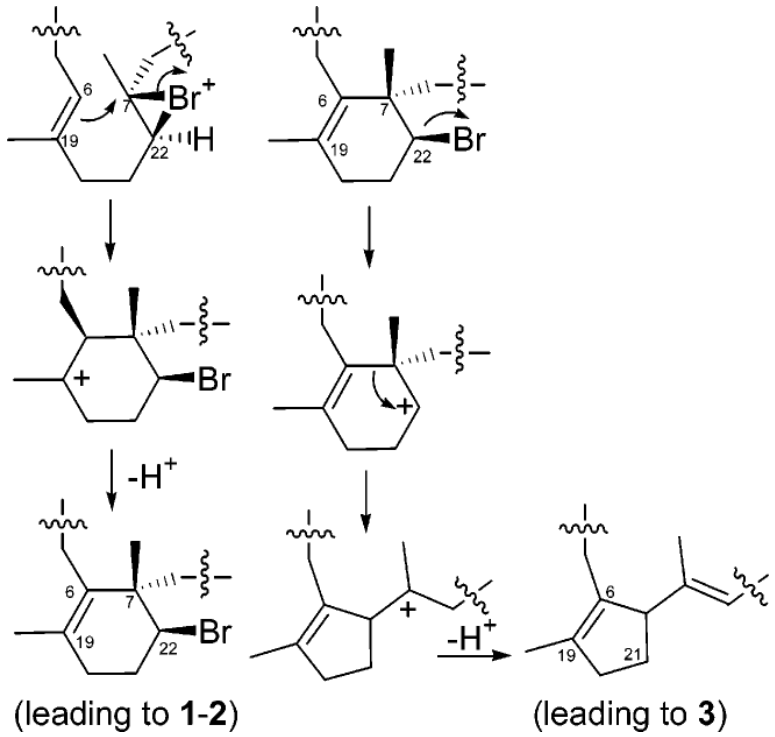

Scheme 1.
Proposed Biogenesis of Diterpene Carbocyclic Rings for **1**–**3**[a]
[a]Atom numbering as in Figure 1.

Org Lett. Author manuscript; available in PMC 2012 June 14.

Table 1

^{13}C and ^{1}H NMR Spectral Data for **1**–**3** (500 MHz; in $CDCl_3$)[a]

	1		2		3	
no.	**δ ^{13}C**	**δ ^{1}H ($^{3}J_{H,H}$)**	**δ ^{13}C**	**δ ^{1}H ($^{3}J_{H,H}$)**	**δ ^{13}C**	**δ ^{1}H ($^{3}J_{H,H}$)**
1	165.9		165.1		166.8	
2	121.5		123.6		122.8	
3	131.4	7.97 d (<2.0)	130.3	7.68 d (<2.0)	133.6	7.64 d (2.0)
4	125.5		126.0		124.3	
5	29.1	3.25 d (18.1)	28.9	3.41 d (18.3)	31.2	3.24 d (14.9)
		3.47 d (18.2)		3.46 d (18.7)		3.58 d (15.1)
6	130.1		130.0		133.0	
7	43.5		43.5		59.8	3.31 m
8	37.6	1.31 m, 1.90 m	38.2	1.66 dd (13.3, 3.4)	138.2	
				1.84 m		
9	28.6	1.77 m	28.9	1.99 m, 2.01 m	122.8	5.28 br d (9.0)
		2.03 m				
10	73.6	3.45 m	68.8	3.63 dd (7.2, 4.4)	27.7	1.72 m, 2.12 m
11	72.5		74.0		59.8	2.91 dd (7.8,2.6)
12	34.3	1.08 m, 1.72 m	36.0	1.45 m, 2.06 m	59.0	
13	28.3	2.05 m, 2.12 m	29.1	2.03 m, 2.16 m	31.8	1.80 m, 2.06 m
14	80.4	4.65 dd (10.9, 1.9)	61.6	4.47 m	20.9	1.58 m, 1.77 m
15	67.3		83.4		81.7	4.96 dd (10.7, 2.2)
16	129.8	7.82 dd (8.3, 1.9)	129.5	7.78 dd (8.3, 1.8)	130.5	7.83 dd (8.5, 2.1)
17	115.2	6.83 d (8.3)	115.1	6.79 d (8.3)	116.0	6.81 d (8.4)
18	158.1		157.8		159.5	
19	133.5		132.7		138.0	
20	33.6	2.02 m, 2.30 m	32.1	2.22 m	37.5	2.33 m, 2.39 m
21	30.5	2.28 m	29.4	2.22 m, 2.35 m	26.2	1.59 m, 1.91 m
22	60.9	4.48 dd (10.8, 4.0)	61.6	4.47 m	14.4	1.92 s
23	21.0	1.40 s	21.1	1.47 s	11.4	0.93 s
24	26.1	1.30 s	25.4	1.25 s	19.2	1.17 s

	1		2		3	
no.	**δ ^{13}C**	**δ ^{1}H ($^{3}J_{H,H}$)**	**δ ^{13}C**	**δ ^{1}H ($^{3}J_{H,H}$)**	**δ ^{13}C**	**δ ^{1}H ($^{3}J_{H,H}$)**
25	33.7	1.28 s	28.5	1.25 s	72.6	
26	30.9	1.81 s	24.2	1.69 s	25.2	1.23 s
27	31.6	1.80 s	26.1	1.82 s	26.4	1.24 s
OH		5.55 br s		5.52 br s		5.80 s
OH		1.96 br s				

[a]Key: br = broad; s = singlet; d = doublet; dd = doublet of doublets; m = multiplet.

Org Lett. Author manuscript; available in PMC 2012 June 14.

Table 2

Pharmacological Activities of **1**–**3**

	antibacterial MIC[c] (μM)		anticancer activity		anti-HIV IC_{50} (μM)		
compd	**MRSA**	**VREF**	**IC_{50} (μM)[a]**	**cell line selectivity (max IC_{50}/min IC_{50})**	**HIV-1 strain 96USHIPS7**	**HIV-1 strain UG/92/029**	**antifungal[b] IC_{50} (μM)**
1	5.9	5.9	6.7	4.8	9.8	9.1	49
2	5.9	3.0	27.7	3.8	NT	NT	49
3	NT	NT	>76		NT	NT	NSA

[a] Mean of 11 cell lines (see the Supporting Information for details).

[b] Using amphotericin B-resistant *Candida albicans*.

[c] MRSA = methicillin-resistant *Staphylococcus aureus*; VREF = vancomycin-resistant *Enterococcus faecium*; NSA indicates not significantly active; NT indicates not tested.

Org Lett. Author manuscript; available in PMC 2012 June 14.

Table 3

Effect of Bromophycolide A (**1**) on Cell Cycle Progression and Induction of Apoptosis

treatment	% apoptosis	% G1	% S	% G2/M
control	1.5	43.7	41.9	12.7
compound **1** (3 μM)	3.0	52.1	32.3	13.5
compound **1** (10 μM)	19.3	56.7	27.9	6.7